Published in final edited form as:
Biochem Pharmacol. 2013 January 1; 85(1): 46–58. doi:10.1016/j.bcp.2012.10.007.

Growth differentiation factor 15 stimulates rapamycin-sensitive ovarian cancer cell growth and invasion

Samantha E. Griner[a,c], **Jayashree P. Joshi**[a,c], and **Rita Nahta**[a,b,c,d,*]

[a]Department of Pharmacology, School of Medicine, Emory University, Atlanta, GA 30322, United States

[b]Department of Hematology & Medical Oncology, School of Medicine, Emory University, Atlanta, GA 30322, United States

[c]Winship Cancer Institute, Emory University, Atlanta, GA 30322, United States

[d]Graduate Division of Biological and Biomedical Sciences, Emory University, Atlanta, GA 30322, United States

Abstract

Identification of novel molecular markers and therapeutic targets may improve survival rates for patients with ovarian cancer. In the current study, immunohistochemical (IHC) analysis of two human ovarian tumor tissue arrays showed high staining for GDF15 in a majority of tissues. Exogenous stimulation of ovarian cancer cell lines with recombinant human GDF15 (rhGDF15) or stable overexpression of a GDF15 expression plasmid promoted anchorage-independent growth, increased invasion, and up-regulation of matrix metalloproteinases (MMPs) and vascular endothelial growth factor (VEGF). MMP inhibition suppressed GDF15-mediated invasion. In addition, IHC analysis of human ovarian tumor tissue arrays indicated that GDF15 expression correlated significantly with high MMP2 and MMP9 expression. Exogenous and endogenous GDF15 over-expression stimulated phosphorylation of p38, Erk1/2, and Akt. Pharmacologic inhibition of p38, MEK, or PI3K suppressed GDF15-stimulated growth. Further, proliferation, growth, and invasion of GDF15 stable clones were blocked by rapamycin. IHC analysis demonstrated significant correlation between GDF15 expression and phosphorylation of mTOR. Finally, knockdown of endogenous GDF15 or neutralization of secreted GDF15 suppressed invasion and growth of a GDF15-over-expressing ovarian cancer cell line. These data indicate that GDF15 over-expression, which occurred in a majority of human ovarian cancers, promoted rapamycin-sensitive invasion and growth of ovarian cancer cells. Inhibition of mTOR may be an effective therapeutic strategy for ovarian cancers that over-express GDF15. Future studies should examine GDF15 as a novel molecular target for blocking ovarian cancer progression.

*Corresponding author at: Department of Pharmacology, Emory University, Suite 5001, 1510 Clifton Rd., Atlanta, GA 30322, United States. Tel.: +1 404 778 3097; fax: +1 404 778 5530. rnahta@emory.edu (R. Nahta).

Keywords

GDF15; mTOR; PI3K; Ovarian cancer; Invasion; Rapamycin

1. Introduction

Increased circulating levels of growth differentiation factor 15 (GDF15) have been associated clinically with disease progression in several solid tumor types [1–5]. Knockdown of GDF15 reduced growth of brain tumor and breast cancer cell lines or xenograft models [3,6]. Recently, GDF15 was reported as being overexpressed in serum samples and tumor lysates collected from patients with advanced ovarian cancer in contrast to patients with benign ovarian cysts or healthy control subjects [4,7]. However, the molecular mechanisms by which GDF15 contributes to ovarian cancer progression were not addressed, and studies examining whether GDF15 inhibition suppresses growth or invasion of ovarian cancer have not yet been reported.

Activation of the PI3K/mTOR signaling pathway has been documented in a majority of ovarian cancers. In one study, primary human ovarian tumors and solid metastases showed frequent phosphorylation of Akt (99% of samples) and mTOR (93% of samples) [8]. In another study, mTOR was found to be phosphorylated in 86% of human clear cell carcinomas and 50% of human serous adenocarcinomas of the ovary [9]. Activation of PI3K/mTOR in ovarian cancer correlated with poor prognostic indicators including advanced stage, histologic grade, and residual mass [8,10].

In the current study, we tested the hypothesis that GDF15 stimulates growth and invasion of ovarian cancer cells. Our data suggest that GDF15 stimulates ovarian cancer cell growth and invasion through mechanisms involving PI3K/mTOR and MAPK signaling. Importantly, GDF15 over-expression was detected in a majority of human ovarian tumor tissues in association with high levels of MMP2, MMP9, and phosphorylated mTOR. Inhibition of mTOR-MMP signaling using rapamycin or the pan-MMP inhibitor GM6001 blocked GDF15-mediated invasion. In addition, GDF15 knockdown or neutralization suppressed growth and invasion of GDF15-over-expressing ovarian cancer cells. These studies support further pre-clinical investigation of GDF15 as a potential mediator of ovarian cancer growth and invasion.

2. Materials and methods

2.1. Materials

Recombinant human GDF15 (rhGDF15; R&D Systems, 614 McKinley Place NE, Minneapolis, MN 55413) was dissolved in 4 mM HCl containing 0.1% BSA; the solvent (HCl-BSA) was used as vehicle control. Pan-MMP inhibitor GM6001 (EMD Millipore, 290 Concord Road, Billerica, MA 01821) was dissolved in DMS0 as a 10 mM stock. LY294002 PI3K inhibitor (EMD Millipore) was dissolved in DMSO to a final concentration of 50 mM. PD0325901 MEK inhibitor (Cayman Chemical, 1180 East Ellsworth Road, Ann Arbor, MI 48108) was dissolved in DMSO to a final concentration of 2 mM. SB203580 p38MAPK

inhibitor (Sigma–Aldrich, 3050 Spruce St., St. Louis, MO 63103) was dissolved in DMSO to a final concentration of 100 mM. Rapamycin mTOR inhibitor (Sigma–Aldrich) was supplied as a 2.74 mM solution in DMSO. TGF beta receptor type II inhibitor SB431542 (Sigma–Aldrich) was dissolved in DMSO as a 10 mM stock.

2.2. Immunohistochemistry (IHC)

IHC was performed on 2 sets of human ovarian tumor tissue microarrays (TMA) using a standard immunoperoxidase procedure. The first TMA consisted of 5 normal and 29 ovarian cancer tissues (Origene, 9620 Medical Center Dr., Suite 200, Rockville, MD 20850). The second TMA consisted of 122 ovarian cancer tissues (representing 61 patients, with two different cores from each patient, giving a total of 122 ovarian tumor tissues), and 10 non-cancerous ovarian tissues (representing 5 subjects, with two different tissue sections from each subject) (Biochain Institute, 39600 Eureka Drive, Newark, CA 94560). The tissue sections on glass slide were deparaffinized by heating at 60 °C, followed by passages through xylene and alcohol grades, and ultimately to water. Antigen retrieval was performed by boiling the slides in 10 mM citrate buffer, pH 6.0 for 10 minutes (min), followed by cooling in the same buffer for 30 min. The endogenous peroxidase was quenched by incubating slides with 0.3% H_2O_2 in methanol for 15 min. Following washes with water and PBS/TBS, slides were incubated in 10% swine serum (Dako North America, Inc., 6392 Via Real, Carpinteria, CA 93013) for 1 hour (h) to eliminate any nonspecific background staining. Tissue sections were stained for human GDF15 (3249, dilution 1:100; Cell Signaling Technology, Inc., 3 Trask Lane, Danvers, MA 01923), MMP2 (37150, dilution 1:500; AbCam, 1 Kendall Square, Suite B2304, Cambridge, MA 02139-1517), MMP9 (3852, dilution 1:500; Cell Signaling), or p-S2448 mTOR (2976, dilution 1:75; Cell Signaling) overnight at 4 °C. Biotinylated anti-rabbit antibody (Dako) was used as secondary antibody, and positive staining was detected by incubation with 3,3-diaminobenzidine solution (DAB+ chromogen; Dako North America, Inc.) with hematoxylin as a counterstain. The slides were then washed in water and dehydrated by passing through alcohol grades and xylene. The slides were mounted with permanent mounting medium Permount (Fisher Scientific, 300 Industry Dr., Pittsburgh, PA 15275). After drying completely, the slides were viewed under a light microscope and pictures were taken at 10×.

2.3. Cell culture

CaOv3, OvCar3, SKOv3, and Tov21G ovarian cancer cells were purchased from American Type Culture Collection (10801 University Boulevard, Manassas, VA 20110). Culture conditions were: SKOv3 in RPMI + 10% FBS; OvCar3 in RPMI + 20% FBS, 1% glutamine, and 0.01 mg/mL bovine insulin; CaOv3 in DMEM + 10% FBS; TOV21G in 45% Medium 199, 45% MCB105, 10% FBS. All media was supplemented with 1% penicillin/streptomycin. Stable transfectants were developed by transfecting empty pCMV vector or GDF15 expression plasmid (Origene) into SKOv3 using Lipofectamine transfection reagent. After 24 h, 200 μg/mL G418 was added to cultures to select for transfectants. GDF15 stable clones and control clones were isolated and tested by real-time PCR for GDF15 expression normalized to RPLPO internal control; stable transfection was verified by real-time PCR in triplicate cultures per clone at least 3 times with reproducible results.

2.3.1. Lentiviral shRNA infection—Lentiviral shRNA construct for GDF15 or control shRNA in pLKO.1 vector was purchased from Open Biosystems (RHS4078; 2650 Crescent Dr., Suite 100, Lafayette, CO 80026). Lentiviral helper plasmids (pCMV-dR8.2 dvpr and pCMV-VSV-G) were obtained from Addgene (8455 and 8454) (1 Kendall Square, Suite B7102, Cambridge, MA 02139). Transient lentivirus stocks were prepared following the manufacturer's protocol. Briefly, 2.5×10^6 293 T cells were plated in 10 cm dishes. Cells were cotransfected with shRNA construct (3 μg) together with 3 μg pCMV-dR8.2 dvpr and 0.3 μg pCMV-VSV-G helper constructs. Culture medium containing virus was harvested every 24 h for 72 h, and centrifuged 10,000 × *g* overnight at 4 °C. Concentrated viral supernatant was collected. Tov21G cells were plated in normal media and infected with purified virus for 36 h.

2.3.2. Anchorage-independent growth—Cells were plated in matrigel (BD Biosciences, 2350 Qume Drive, San Jose, CA 95131) diluted 1:1 (media: matrigel). The matrigel-cell suspension was allowed to solidify, and then media containing rhGDF15, vehicle control, and/or various drugs (depending on the experiment) was added to cells in triplicate cultures. Media, rhGDF15, and drugs were renewed twice a week for 3–4 weeks. Photographs were taken with an Olympus IX50 inverted microscope at 4× magnification. Matrigel was digested using dispase (BD Biosciences), and viable cells were counted by trypan blue exclusion. Average cell viability of triplicates and standard deviation between triplicates was calculated. Experiments were performed twice with reproducible results.

2.3.3. Invasion chamber assays—SKOv3 parental, stable clone, stable GDF15-expressing cells (5×10^4 cells/mL), or TOV21G (1×10^5 cells/mL) were plated in serum-free media in BD Biosciences BioCoat Matrigel Invasion Chambers with 0.75 mL of chemoattractant, which was culture media containing 10% FBS ± 20 ng/mL rhGDF15. Depending on the experiment, vehicle control, rapamycin (100 nM), control human IgG or GDF15 mAb (1 μg/mL) were added directly to chambers. After 24 h, non-invading cells were removed from the interior surface of the membrane by scrubbing gently with dry cotton tipped swab. Each insert was then transferred into 100% methanol for 2 min followed by H&E staining. The chambers were incubated with hematoxylin for 6 min followed by acid alcohol and bluing agent to stain nuclei. Further the slides were incubated in eosin to stain cytoplasm for 2 min. The slides were then washed in water and dehydrated by passing through alcohol grades. The slides were mounted with Permount. Photographs were taken of 10 fields at 20× magnification per sample, with triplicates performed per treatment group. The number of cells was counted in each field; the sum total of the 10 fields was calculated for each sample. Experiments were performed at least twice with reproducible results.

2.3.4. Real-Time Cell Analysis—Cell growth was monitored in real time using a Real-Time Cell Analyzer Dual-Plate (RTCA DP) instrument (Roche Applied Science, P.O. Box 50414, 9115 Hague Road, Indianapolis, IN 46250-0414), placed in a humidified incubator maintained at a 5% CO_2 and 37 °C. The RTCA DP system records cell index (CI) as a unit-less number that is a function of electrical impedance of cells attached to interdigitated electrodes built into the bottom of wells of a 16-well E-plate (Roche Applied Science). Recording of CI as well as subsequent data analysis were performed using the RTCA

Software 1.2 (Roche Applied Science). Background impedance in each well in the presence of media alone was measured prior to cell seeding and automatically subtracted by the RTCA software. For anchorage-dependent proliferation assays, 5000 cells/well were seeded in Eplates with 10% FBS containing medium, plus 20 ng/mL rhGDF15 where indicated. CI was recorded every 15 min for 24 h. Assays were performed at least twice with reproducible results. Cell migration was assessed using double-chamber 16-well plates with microelectrodes located on the underside of the upper chamber's PET membrane containing 8.1 m pores (CIM-plate 16, Roche Applied Science). Medium containing 10% FBS was added to the lower chamber, with 20 ng/mL rhGDF15 where indicated, and cells were seeded in the upper chamber at 30,000 cells/well in medium containing 5% FBS with 100 nM rapamycin where indicated. The CIM-plate 16 was monitored every 15 min for the next 10 h. Assays were performed at least twice with reproducible results.

2.4. Real-time PCR

Total RNA was extracted using the RNeasy purification kit (Qiagen, 27220 Turnberry Lane, Valencia, CA 91355) and DNase treated (Invitrogen). cDNA was then prepared from total RNA using random primers and the Superscript III first strand synthesis Kit (Invitrogen). Relative levels of mRNA were determined by real-time quantitative PCR using an Eppendorf cycler and the TaqMan Universal PCR master Mix (4304437, Applied Biosystems, 5791 Van Allen Way, P.O. Box 6482, Carlsbad, CA 92008); RPLPO mRNA levels were used for normalization. Primers for GDF15 (Hs00171132_m1), MMP-2 (Hs-01548725_m1), MMP-9 (Hs00957555_m1), VEGF (Hs00153458_m1), and RPLPO (Hs99999902_m1) were obtained from Applied Biosystems (Taq-Man Gene Expression Assays). Samples were normalized against the RPLPO internal control and compared as arbitrary units, represented as mean ± SD. Samples were run in triplicate, and experiments were repeated at least 3 times with reproducible results.

2.5. ELISA

Human GDF15 immunoassay (R&D Systems) was used according to the manufacturer's directions. Briefly, sample media was incubated in GDF15 antibody-coated microplates for 2 h, then washed and incubated with GDF15 antibody conjugated to horseradish peroxidase for 1 h. After washing, plates were incubated with color reagent (hydrogen peroxide–chromogen mix) for 30 min. Optical density of each well was determined using a microplate reader set to 450 nm. The concentrations were calculated according to the standards supplied with the kit by creating a four parameter logistic curve-fit. Samples were run in triplicate, and experiments were repeated 3 times with reproducible results.

2.6. Western blotting

Cells were lysed in RIPA buffer (Cell Signaling) supplemented with protease and phosphatase inhibitors (Sigma). Total protein extracts were run on SDS-PAGE and blotted onto nitrocellulose. Blots were probed overnight using the following antibodies: from Cell Signaling, monoclonal p-S473 Akt-XP (1:1000), and polyclonal antibodies against: total Akt (1:1000), p-Thr202/Tyr204 p42/p44 Erk1/2 (1:1000), total p42/p44 Erk1/2 (1:1000), p-Thr180/Tyr182 p38 XP (1:1000), p-Thr 37/46 4EBP1 (1:1000), total 4EBP1 (1:1000), N-Cadherin (1:1000). In addition, polyclonal p38 (1:1000) from EMD Biosciences and β-actin

monoclonal AC-15 (Sigma) at 1:10,000. Protein bands were detected using the Odyssey Imaging System (Li-Cor Biosciences, 4647 Superior Street, Lincoln, NE 68504-1357). Quantification of bands was determined using ImageJ software.

2.7. Statistics

p-Values were determined for experimental versus control treatments by two-tailed Student's *t*-test, $*p < 0.05$, $**p < 0.005$. IHC staining correlations were determined by two-tailed Fisher's exact test.

3. Results

3.1. GDF15 is over-expressed in a majority of human ovarian tumor tissues

Elevated expression of GDF15 was previously reported in serum and tumor samples of patients with ovarian cancer [4,7]. To obtain further evidence that GDF15 expression is increased in ovarian cancer, we performed IHC on two commercially available human ovarian tumor tissue arrays (Fig. 1). On the first tumor array, 21 of 29 (72.4%) tumor tissues showed GDF15-positive staining, as compared to 5 non-cancerous tissue samples, none of which stained positive for GDF15 (Table 1). On the second array, 101 of 122 (82.79%) tumor tissues showed GDF15-positive staining (Table 2), with the most common subtype of ovarian cancer, the serous subtype, showing over-expression of GDF15 in the vast majority of samples (45 of 47, or 95.7%). Endometrioid and mucinous subtypes also showed elevated GDF15 expression in the majority of cases, with 80.4% and 62.5%, respectively, showing high GDF15 staining. Thus, GDF15 was over-expressed in the vast majority of ovarian cancer tissues on two different arrays.

3.2. GDF15 stimulates anchorage-independent growth of ovarian cancer cells

Since the majority of ovarian tumor tissues expressed GDF15, we examined the biological effects of increasing GDF15 expression in ovarian cancer cell lines. SKOv3, OvCar3, and CaOv3 ovarian cancer cell lines secrete relatively low levels of GDF15 (Fig. 2A), so we used these lines to examine biological effects of exogenous stimulation with recombinant human GDF15 (rhGDF15). Cells were grown in three-dimensional cultures supplemented with 20 ng/mL of rhGDF15, a physiologically relevant concentration found in the serum of patients with ovarian cancer [4]. Exposure to rhGDF15 caused a statistically significant increase in anchorage-independent growth of ovarian cancer cells (Fig. 2B). Cells that were grown in rhGDF15 showed projections in contrast to control cultures, suggestive of increased invasiveness. In addition to stimulating with recombinant cytokine, we stably transfected a GDF15 expression plasmid into SKOv3 cells (Fig. 2C). GDF15 stable transfectants showed increased growth in matrigel relative to control clones (Fig. 2D). Real time cell analysis, which has tight reproducibility with traditional MTS and trypan blue assays [11–13], but allows the additional advantage of monitoring growth, proliferation, or migration in real time over a selected period rather than at one time point, was used here to obtain additional confirmation of the growth-promoting effects of GDF15 in ovarian cancer cells. Cell count profiles (the number of cells over time) were determined for SKOv3 parental cells stimulated with vehicle control or rhGDF15, and for stable empty vector control and stable GDF15-transfected clones over a 24 h period (Fig. 2E). GDF15 stable

clones showed an increased number of cells relative to control stable or parental cells, and rhGDF15-stimulated cells showed an increased number of cells versus vehicle control-stimulated parental cells. Collectively, the matrigel growth and real time cell assays demonstrated that GDF15 stimulates growth and an increase in the number of ovarian cancer cells over time.

3.3. GDF15 increases invasiveness of ovarian cancer cells

Next, SKOv3 cells were plated in matrigel-coated Boyden chambers, and stimulated with vehicle control or rhGDF15. Exposure to rhGDF15 caused a dramatic increase in invasiveness of SKOv3 cells (Fig. 3A). Similarly, GDF15-over-expressing stable clones showed a significant increase in invasiveness through Boyden chambers compared to control clone cells (Fig. 3B). Increased invasiveness of cancer cells is often associated with an epithelial to mesenchymal transition (EMT). GDF15 stable clones showed morphologic changes representative of transition to a mesenchymal phenotype (Fig. 3C). GDF15 stable clones showed a more elongated appearance relative to the control clone, which showed a more cuboidal phenotype. Western blotting further suggested EMT in GDF15 stable clones, as the mesenchymal marker N-cadherin was markedly up-regulated in the presence of stable over-expression of GDF15. In addition to invasion through Boyden chambers, we examined cell migration through a polyethylene terephtalate (PET) membrane using real time cell analysis XCelligence assay. Consistent with matrigel invasion assays, stimulation with rhGDF15 or stable over-expression of GDF15 led to increased migration of ovarian cancer cells in real time assays (Fig. 3D).

MMP2, MMP9, and VEGF have previously been reported to mediate ovarian cancer cell invasion [14–16]. Real-time PCR showed increased expression of MMP2, MMP9, and VEGF in GDF15 stable clones relative to control clone cells (Fig. 3E). In addition, IHC analysis of human ovarian tumor arrays showed strong staining for MMP2 and MMP9 in a majority of tumor tissues (Fig. 3F). GDF15 expression was significantly correlated with expression of MMP2 and MMP9 (Table 3), supporting the concept that GDF15 overexpression is associated with increased expression of mediators of invasion. To determine if increased expression of MMPs contributes to GDF15-stimulated ovarian cancer cell invasion, we treated GDF15 stable clones with the pan-MMP inhibitor GM6001. Pharmacologic inhibition of MMPs suppressed invasiveness of GDF15-over-expressing cells (Fig. 3G). These results indicate that GDF15 stimulates ovarian cancer cell invasion through a mechanism involving MMPs.

3.4. PI3K/MAPK signaling contributes to GDF15-stimulated growth of ovarian cancer cells

Based on reports that PI3K activation contributes to ovarian cancer progression, we performed Western blotting for PI3K and MAPK signaling molecules in cells stimulated with rhGDF15. These blots indicated that rhGDF15 induced phosphorylation of p38MAPK, Erk1/2, and Akt within 2 min of stimulation in SKOv3 and CaOv3 cells (Fig. 4A). To determine if activation of these signaling pathways is required for GDF15-mediated growth, ovarian cancer cells were stimulated with rhGDF15 in the presence of pharmacological inhibitors of PI3K (LY294002), p38 (SB203580), or MEK (PD0325901). The increase in anchorage-independent growth that was stimulated by rhGDF15 was overcome by each of

the kinase inhibitors (Fig. 4B). These results suggest that PI3K and MAPK activation contribute to GDF15-stimulated growth of ovarian cancer cells.

3.5. Inhibition of mTOR suppresses proliferation and growth of GDF15 stable clones

Next, we examined PI3K and MAPK signaling in stable GDF15-over-expressing clones. Stable clones showed increased phosphorylation of p38, Akt, and 4EBP1 with slight variability between individual clones (Fig. 4C). To determine if mTORc1 signaling is important for GDF15-mediated biological effects in ovarian cancer, we treated GDF15 stable clones with the mTORc1 inhibitor rapamycin. Stable GDF15 clones showed dose-dependent inhibition of proliferation in response to rapamycin in contrast to control cells (Fig. 4D). This increased sensitivity to rapamycin suggests that GDF15-over-expressing ovarian cancer stable clones may have acquired dependence upon mTORc1 signaling. Since GDF15 is structurally related to TGF beta, we also treated stable GDF15 clones with the TGF beta receptor type II inhibitor SB431542. In contrast to rapamycin, TGF beta receptor inhibition did not affect proliferation of GDF15 stable clones, suggesting that proliferation of GDF15 clones is not dependent upon TGF beta signaling. Consistent with these findings, GDF15-mediated anchorageindependent growth of ovarian cancer cells was blocked by mTOR inhibitor rapamycin, but not by TGF beta receptor inhibitor SB431542 (Fig. 4E). Finally, since inhibition of PI3K, MEK, and p38MAPK reduced GDF15-stimulated anchorage-independent growth of ovarian cancer cells (Fig. 4B), we examined whether inhibitors of these pathways also reduced anchorage-dependent proliferation of GDF15 stable clones. In contrast to mTOR inhibition, clones did not show increased sensitivity to pharmacological inhibition of PI3K (LY294002), MEK (PD0325901), or p38MAPK (SB203580) relative to empty vector control (Fig. 4F).

3.6. Inhibition of mTOR suppresses GDF15-mediated invasion in ovarian cancer cells

Since GDF15 clones showed heightened sensitivity to rapamycin in MTS assays, we performed Boyden chamber assays to determine if rapamycin also inhibits GDF15-mediated invasion. The increased invasiveness of SKOv3 cells that was stimulated by rhGDF15 was suppressed by rapamycin (Fig. 5A). Rapamycin also reduced rhGDF15-stimulated expression of the invasion markers MMP9 and VEGF (Fig. 5B). Similarly, invasiveness of GDF15 stable clones through matrigel-coated Boyden chambers was significantly reduced by rapamycin (Fig. 5C). Consistent with these results, real time cell analysis indicated that migration of GDF15-over-expressing stable clones and rhGDF15-stimulated SKOv3 cells was inhibited by rapamycin (Fig. 5D). Finally, to determine if mTOR signaling and GDF15 are associated in human tumor samples, we used the same tumor tissue array as in Table 2, and performed IHC staining for phospho-S2448 mTOR (Fig. 5E). Positive staining for phosphorylated mTOR showed significant correlation with positive staining for GDF15 (Table 4). These data indicate that GDF15 expression is associated with mTOR activation in human ovarian tumor tissues.

3.7. GDF15 pharmacologic inhibition or knockdown reduces growth and invasion in an ovarian cancer model of endogenous GDF15 overexpression

GDF15-specific ELISA showed that Tov21 ovarian cancer cells secrete 33-fold higher levels of GDF15 compared to SKOv3 cells (Fig. 6A). Treatment of Tov21 cells with GDF15

monoclonal antibody (mAb) clone 147627 (R&D Systems) resulted in neutralization of secreted GDF15 as compared to control IgGtreated or untreated cells (Fig. 6B). GDF15 mAb also reduced expression of MMP2, MMP9, and VEGF transcripts (Fig. 6C), suppressed growth in matrigel (Fig. 6D), and blocked invasiveness (Fig. 6E) of Tov21 cells compared to control IgG-treated cells.

Real-time PCR indicated that endogenous expression of the GDF15 transcript was increased in Tov21 by approximately 7-fold relative to SKOv3 cells (Fig. 7A). GDF15 expression was knocked down using lentiviral GDF15 shRNA (Fig. 7B), which also resulted in reduced expression of MMP2, MMP9, and VEGF transcripts (Fig. 7C). GDF15 knockdown reduced growth in matrigel (Fig. 7D) and invasiveness (Fig. 7E) of Tov21 cells relative to control shRNA-infected cells. Knockdown of GDF15 reduced the ratio of phosphorylated to total 4EBP1 and p38, with a slight reduction in phosphorylated to total Erk1/2 also observed (Fig. 7F). In contrast, phosphorylation of Akt was not reduced. These results suggest that GDF15 knockdown reduces mTOR and MAPK signaling and suppresses growth and invasion of Tov21 ovarian cancer cells. The lack of effect on Akt phosphorylation as well as the modest effect on Erk1/2 may have been due to our ability to achieve only a partial knockdown (Fig. 7B). Future studies will attempt to develop knockdown strategies that achieve greater suppression of GDF15, and will then determine if PI3K and MAPK signaling are reduced to a greater extent when expression of endogenous GDF15 is more completely blocked.

4. Discussion

Ovarian cancer is the leading cause of death from gynecologic tumors in the United States. Approximately 22,000 women will be diagnosed with ovarian cancer this year, with 15,000 dying from the disease [17]. Most cases are diagnosed at a late stage, and generally carry a poor prognosis as they have already spread outside of the ovary. Identification of a biomarker for ovarian cancer may facilitate diagnosis at an earlier stage, and could provide a new molecular target for blocking metastatic spread.

In the current study, we show that the cytokine GDF15 was expressed at high levels in 70–80% of all ovarian tumors. Approximately 96% of serous tumors, the most common subtype of ovarian cancer, showed elevated GDF15 expression. Bock et al. [7] previously reported that 97% (111 of 114) of ovarian tumors showed cytoplasmic staining for GDF15. In that study, high GDF15 staining correlated with reduced overall survival. Similarly, Staff et al. [4] reported that high plasma GDF15 levels were an independent predictor of reduced overall survival. GDF15 has been suggested to be a biomarker for several cancer types including pancreatic, prostate, colorectal, and multiple myeloma [1–3,5,18]. Our findings together with those previously reported suggest that GDF15 should be studied further as a potential biomarker of ovarian cancer progression.

Stimulation of ovarian cancer cells with exogenous GDF15 or stable transfection with a GDF15 expression plasmid induced growth and invasion through matrigel. GDF15 caused an increased expression of MMPs, which mediate basement membrane breakdown and invasion. Our results showed that greater than 85% of all of the ovarian tumor tissues stained positive for MMP2 and MMP9, including more than half of the GDF15-negative

samples (Table 3). These results suggest that elevated MMP2 and MMP9 may be a general finding amongst ovarian cancer tissues. In fact, levels of MMP2 and MMP9 have previously been reported to be increased in a majority of patients with ovarian cancer [14,19,20]. Our IHC analysis indicated a significant correlation between GDF15 expression and MMP2 and MMP9 positivity in human ovarian tumors. In addition, pharmacologic MMP inhibition suppressed GDF15-mediated invasion, confirming that GDF15-driven invasion is likely to be MMP-dependent. MMP2 has been shown to be an early regulator of ovarian cancer metastasis, with knockdown or pharmacologic inhibition of MMP2 reducing the number of metastases and tumor weight in an in vivo model of ovarian cancer [21]. Thus, the ability of GDF15 to induce expression of MMPs may be a critical downstream component of its mechanism of invasion.

Several signaling pathways up-regulate expression of MMPs. GDF15 activated PI3K/mTOR and MAPK signaling. Kinase inhibition of these pathways blocked GDF15-mediated growth of ovarian cancer cells. However, proliferation of GDF15 stable transfectants was dependent upon only mTOR signaling, as rapamycin achieved dose-dependent inhibition of proliferation, in contrast to PI3K and MEK inhibition. Rapamycin also suppressed GDF15-mediated growth and invasion, and reduced GDF15-stimulated expression of MMPs. Cancer cell motility and invasion mediated by mTORc1-MMP signaling has been reported [22]. Our results showed that pharmacologic mTORc1 inhibition completely suppressed GDF15-mediated invasion and reduced MMP transcript levels, supporting the concept that mTOR signaling contributes to GDF15-mediated invasion in ovarian cancer cells. In addition, stable transfectants of GDF15 showed increased phosphorylation of the mTORc1 substrate 4EBP1, while lentiviral GDF15 shRNA suppressed phosphorylation of 4EBP1 in Tov21 cells. In contrast to GDF15 stimulation in SKOv3 and CaOv3 cells, GDF15 knockdown did not appear to affect Akt and had a modest effect on Erk1/2 phosphorylation in Tov21 cells, suggesting that Tov21 cells may not require GDF15 for sustained Akt or Erk1/2 signaling. GDF15 showed robust stimulation of p38 phosphorylation, which was reduced upon knockdown of GDF15 in Tov21 cells. Further analysis is required to determine the contribution of p38 signaling to GDF15-mediated growth and invasion, as well as the mechanisms by which p38 is activated by GDF15. As suggested by our data, genetically different cell lines are likely to display differential signaling upon stimulation or knockdown of GDF15. However, the same general signaling trend was observed in the various cell lines.

Our results suggest that GDF15-positive cells may be uniquely dependent upon mTOR signaling versus other signaling pathways, as rapamycin was able to inhibit proliferation, growth, and invasion of GDF15-over-expressing cells. Activation of mTOR signaling has previously been implicated in ovarian cancer progression [8,9]. Several analogs of rapamycin are currently in clinical development for treating multiple types of cancer. Based on our results, there is rationale to investigate rapamycin analogs in the context of GDF15-over-expressing ovarian cancer.

GDF15 is structurally similar to TGF beta, although a receptor for GDF15 has not yet been identified. GDF15 appears to stimulate phosphorylation of the TGF beta receptor substrate Smad2 [6]. However, pharmacologic inhibition of TGF beta receptor type II did not reduce GDF15-mediated growth in ovarian cancer cells. However, TGF beta receptor signaling is

known to play an integral role in EMT and cancer cell invasion. In fact, our preliminary data showed that GDF15 stable clones adopt a mesenchymal morphology and express elevated levels of the mesenchymal marker Ncadherin. Thus, it is possible that GDF15 promotes an epithelial-tomesenchymal transition in ovarian cancer cells. Future studies will examine the mechanisms by which GDF15 may mediate EMT and invasion, including determining whether TGF beta receptor signaling is involved in this process.

Amongst ovarian cancers that over-express GDF15, strategies that block GDF15 signaling may prove to be beneficial. We used two strategies to inhibit GDF15: knockdown of endogenous GDF15 expression and neutralization of secreted GDF15. Both approaches suppressed growth and invasion of GDF15-overexpressing ovarian cancer cells. GDF15 knockdown reduced phosphorylation of 4EBP1, supporting the concept that mTORc1 signaling is a critical component of the mechanism of GDF15-mediated growth and invasion of ovarian cancer. Future studies will develop strategies for improving knockdown of GDF15, including using nanoparticleconjugated knockdown approaches as we recently published [23] to selectively target tumor cells. These strategies will be examined for their ability to suppress invasion and progression of ovarian cancer in cell culture and animal models.

Overall, our work supports investigation of GDF15 expression or serum level as a potential predictor of ovarian cancer progression. Having a reliable biomarker of disease is critical for facilitating diagnosis of ovarian cancer at an earlier stage and improving survival rates. Our studies suggest that patients with GDF15-over-expressing ovarian cancer may derive benefit from rapamycin-based treatment. This work is of particular significance as it indicates that GDF15-mTOR signaling is a novel mechanism driving ovarian cancer cell invasion, and that pharmacologically targeting GDF15-mTOR signaling may ultimately block ovarian tumor growth and invasion. GDF15-targeted approaches should be studied further in pre-clinical animal models of ovarian cancer. Further understanding of the mechanisms by which GDF15 stimulates mTOR signaling and promotes progression of ovarian cancer may ultimately allow new therapeutic approaches to be developed for patients with ovarian cancer.

Acknowledgements

R. Nahta gratefully acknowledges funding from The Georgia Cancer Coalition Distinguished Cancer Scholars Program, the Winship Breast Program Pilot Award, and NIH P30 CA138292 to Winship Cancer Institute. The authors acknowledge the Winship Cancer Institute Cell Imaging and Microscopy Center.

References

1. Brown DA, Ward RL, Buckhaults P, Liu T, Romans KE, Hawkins NJ, et al. MIC-1 serum level and genotype: associations with progress and prognosis of colorectal carcinoma. Clin Cancer Res. 2003; 9:2642–2650. [PubMed: 12855642]
2. Mimeault M, Batra SK. Divergent molecular mechanisms underlying the pleiotropic functions of macrophage inhibitory cytokine-1 in cancer. J Cell Physiol. 2010; 224:626–635. [PubMed: 20578239]
3. Roth P, Junker M, Tritschler I, Mittelbronn M, Dombrowski Y, Breit SN, et al. GDF-15 contributes to proliferation and immune escape of malignant gliomas. Clin Cancer Res. 2010; 16:3851–3859. [PubMed: 20534737]

4. Staff AC, Bock AJ, Becker C, Kempf T, Wollert KC, Davidson B. Growth differentiation factor-15 as a prognostic biomarker in ovarian cancer. Gynecol Oncol. 2010; 118:237–243. [PubMed: 20576287]

5. Welsh JB, Sapinoso LM, Kern SG, Brown DA, Liu T, Bauskin AR, et al. Large-scale delineation of secreted protein biomarkers overexpressed in cancer tissue and serum. Proc Natl Acad Sci U S A. 2003; 100:3410–3415. [PubMed: 12624183]

6. Joshi JP, Brown NE, Griner SE, Nahta R. Growth differentiation factor 15 (GDF15)-mediated HER2 phosphorylation reduces trastuzumab sensitivity of HER2-overexpressing breast cancer cells. Biochem Pharmacol. 2011; 82:1090–1099. [PubMed: 21803025]

7. Bock AJ, Stavnes HT, Kempf T, Trope CG, Berner A, Davidson B, et al. Expression and clinical role of growth differentiation factor-15 in ovarian carcinoma effusions. Int J Gynecol Cancer. 2010; 20:1448–1455. [PubMed: 21336029]

8. Bunkholt Elstrand M, Dong HP, Odegaard E, Holth A, Elloul S, Reich R, et al. Mammalian target of rapamycin is a biomarker of poor survival in metastatic serous ovarian carcinoma. Hum Pathol. 2010; 41:794–804. [PubMed: 20153512]

9. Mabuchi S, Kawase C, Altomare DA, Morishige K, Sawada K, Hayashi M, et al. mTOR is a promising therapeutic target both in cisplatin-sensitive and cisplatin- resistant clear cell carcinoma of the ovary. Clin Cancer Res. 2009; 15:5404–5413. [PubMed: 19690197]

10. No JH, Jeon YT, Park IA, Kim YB, Kim JW, Park NH, et al. Activation of mTOR signaling pathway associated with adverse prognostic factors of epithelial ovarian cancer. Gynecol Oncol. 2011; 121:8–12. [PubMed: 21276607]

11. Galante D, Corsaro A, Florio T, Vella S, Pagano A, Sbrana F, et al. Differential toxicity, conformation and morphology of typical initial aggregation states of Abeta1-42 and Abetapy3-42 beta-amyloids. Int J Biochem Cell Biol. 2012; 44:2085–2093. [PubMed: 22903022]

12. Kumar B, Yadav A, Lang J, Teknos TN, Kumar P. Dysregulation of microRNA-34a expression in head and neck squamous cell carcinoma promotes tumor growth and tumor angiogenesis. PLoS One. 2012; 7:e37601. [PubMed: 22629428]

13. Stoddart, MJ. Mammalian cell viability: methods and protocols (methods in molecular biology). Stoddart, MJ., editor. New York: Humana Press; 2011. p. 251

14. Belotti D, Paganoni P, Manenti L, Garofalo A, Marchini S, Taraboletti G, et al. Matrix metalloproteinases (MMP9 and MMP2) induce the release of vascular endothelial growth factor (VEGF) by ovarian carcinoma cells: implications for ascites formation. Cancer Res. 2003; 63:5224–5229. [PubMed: 14500349]

15. Wang FQ, So J, Reierstad S, Fishman DA. Vascular endothelial growth factorregulated ovarian cancer invasion and migration involves expression and activation of matrix metalloproteinases. Int J Cancer. 2006; 118:879–888. [PubMed: 16152587]

16. Zhang A, Meng L, Wang Q, Xi L, Chen G, Wang S, et al. Enhanced in vitro invasiveness of ovarian cancer cells through up-regulation of VEGF and induction of MMP-2. Oncol Rep. 2006; 15:831–836. [PubMed: 16525667]

17. Siegel R, Naishadham D, Jemal A. Cancer statistics**2012. CA Cancer J Clin. 2012; 62:10–29. [PubMed: 22237781]

18. Corre J, Labat E, Espagnolle N, Hebraud B, Avet-Loiseau H, Roussel M, et al. Bioactivity and prognostic significance of growth differentiation factor GDF15 secreted by bone marrow mesenchymal stem cells in multiple myeloma. Cancer Res. 2012; 72:1395–1406. [PubMed: 22301101]

19. Coticchia CM, Curatolo AS, Zurakowski D, Yang J, Daniels KE, Matulonis UA, et al. Urinary MMP-2 and MMP-9 predict the presence of ovarian cancer in women with normal CA125 levels. Gynecol Oncol. 2011; 123:295–300. [PubMed: 21889192]

20. Schmalfeldt B, Prechtel D, Harting K, Spathe K, Rutke S, Konik E, et al. Increased expression of matrix metalloproteinases (MMP)-2, MMP-9, and the urokinase-type plasminogen activator is associated with progression from benign to advanced ovarian cancer. Clin Cancer Res. 2001; 7:2396–2404. [PubMed: 11489818]

21. Kenny HA, Lengyel E. MMP-2 functions as an early response protein in ovarian cancer metastasis. Cell Cycle. 2009; 8:683–688. [PubMed: 19221481]

22. Zhou H, Huang S. Role of mTOR signaling in tumor cell motility, invasion and metastasis. Curr Protein Pept Sci. 2011; 12:30–42. [PubMed: 21190521]

23. Yehl K, Joshi JP, Greene BL, Dyer RB, Nahta R, Salaita K. Catalytic deoxyribozyme- modified nanoparticles for RNAi-independent gene regulation. ACS Nano. 2012; 6:9150–9157. [PubMed: 22966955]

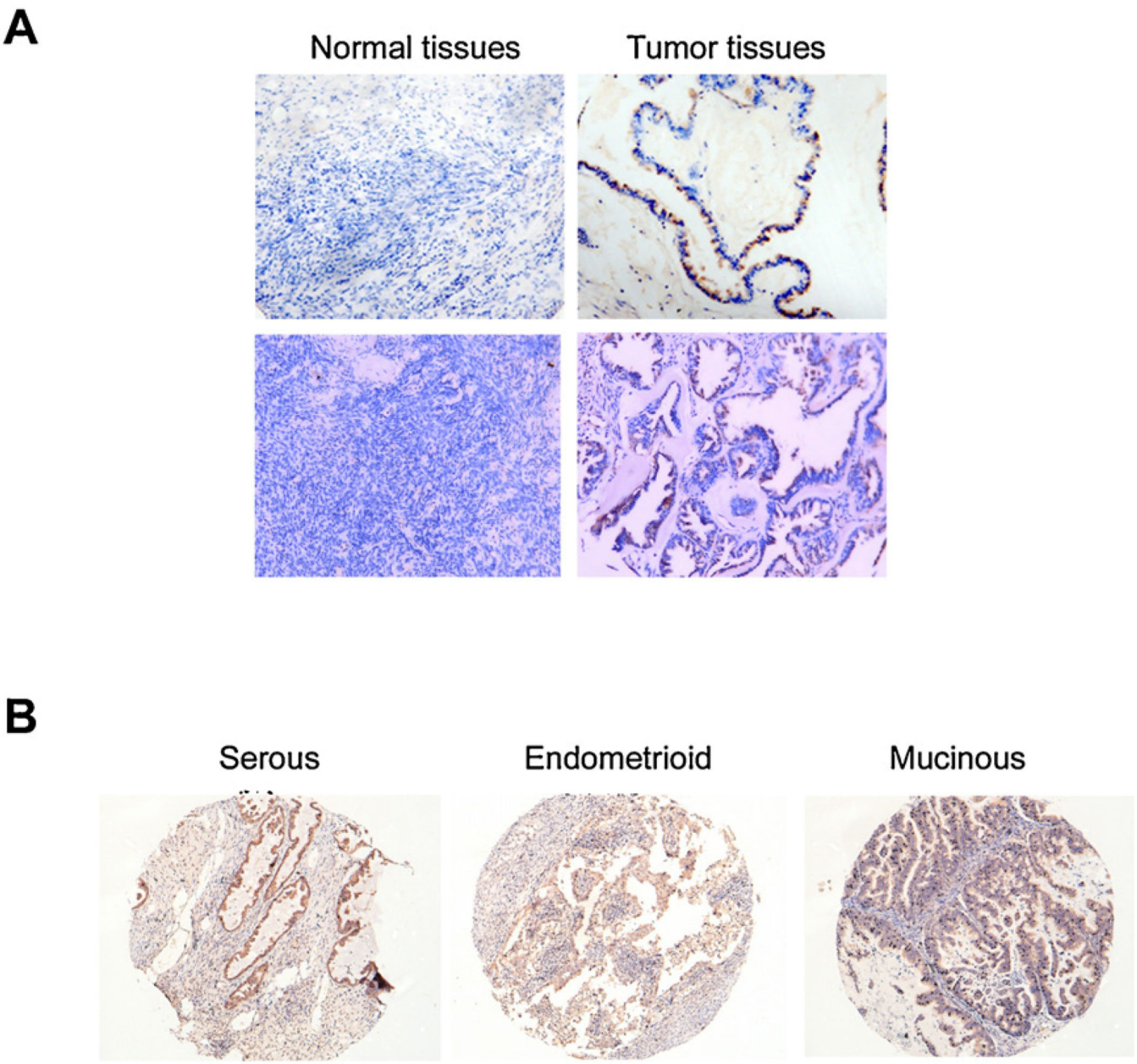

Fig. 1.

IHC for GDF15 on two human ovarian tumor tissue arrays. (A) A tumor tissue array consisting of 29 tumor tissue samples and 5 non-cancerous ovarian tissue samples was stained for GDF15. Photos were taken at 10× magnification under the microscope, and representative photos of 2 normal and 2 tumor tissues are shown. (B) A tumor tissue array consisting of 122 tumor tissues and 10 non-cancerous ovarian tissues was stained for GDF15. This second array included 47 serous, 24 mucinous, and 51 endometrioid ovarian tumor subtype samples. Photos were taken at 5× magnification under the microscope, and representative photos of positive GDF15 staining are shown for each cancer subtype.

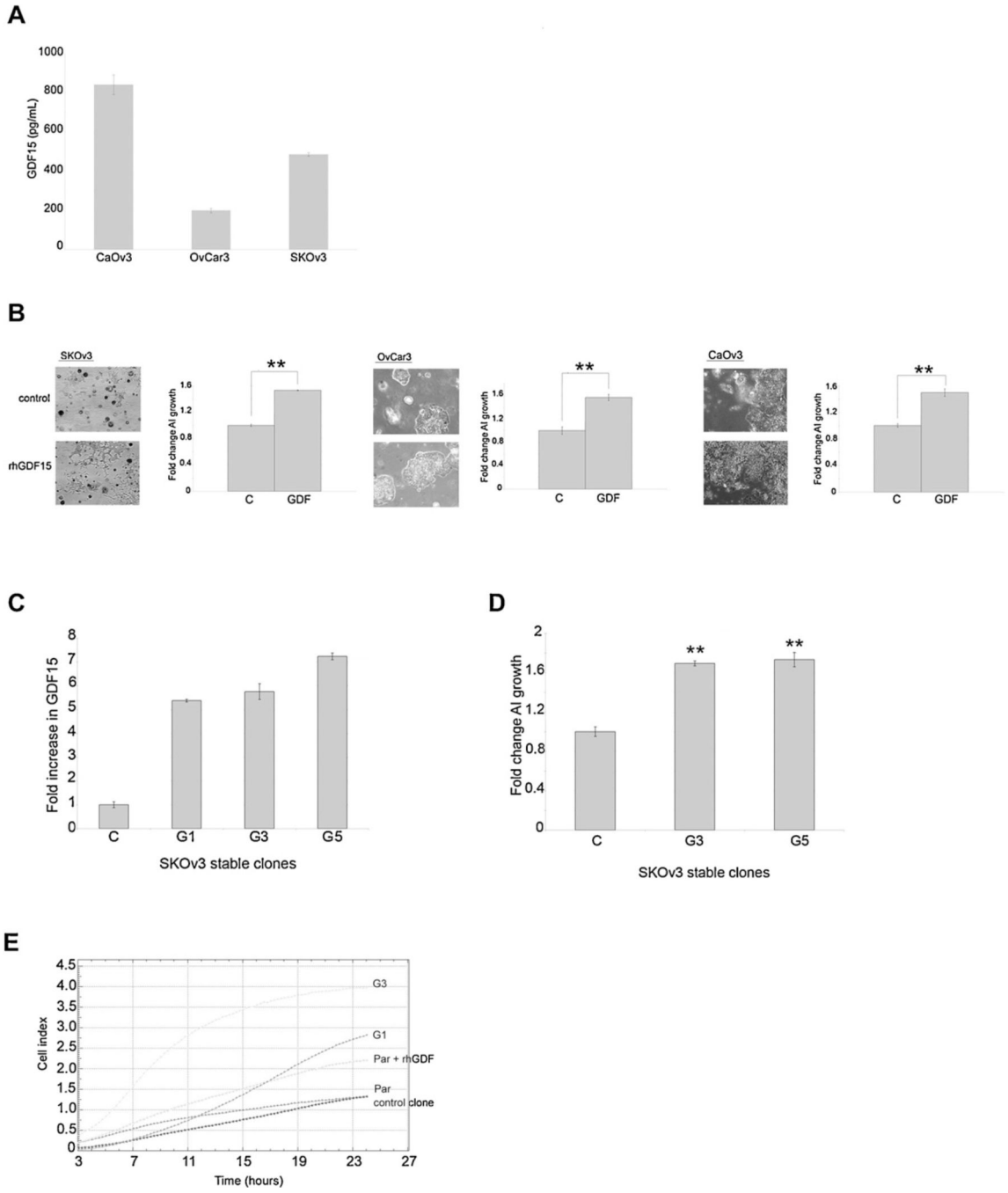

Fig. 2.

GDF15 promotes anchorage-independent growth of ovarian cancer cells. (A) CaOv3, OvCar3, and SKOv3 cells were incubated in serum-free media for 48 h. GDF15 concentration was then determined by ELISA in media from cell lines. (B) SKOv3, OvCar3, and CaOv3 ovarian cancer cells were plated in matrigel, and maintained in media containing 20 ng/mL rhGDF15 or vehicle control. Media was changed twice a week for 3–4 weeks. Representative photographs taken with 4× objective lens are shown. Matrigel was dissolved using dispase and cells were counted by trypan blue exclusion. Average fold change in

anchorage-independent (AI) cell growth is shown for rhGDF15 group (GDF) versus control vehicle group (C) per line. (C) SKOv3 cells were stably transfected with empty vector control or GDF15 expression plasmid. Three GDF15 stable clones (G1, G3, G5) were selected and analyzed by real-time PCR for GDF15 transcript level versus control clone (C). Levels of GDF15 transcript were normalized to RPLPO internal control transcript. Values reflect the average fold change in normalized GDF15 transcript expression per stable clone relative to control clone. (D) Control clone (C) and two GDF15 stable clones (G3 and G5) were plated in matrigel. Media was changed twice a week for 3–4 weeks. Matrigel was then dissolved using dispase and cells were counted by trypan blue exclusion. Average fold change in anchorage-independent (AI) growth is shown for the GDF15 clones relative to control clone. (E) Growth of SKOv3 parental cells treated with vehicle control or 20 ng/mL rhGDF15, or stable control clone or GDF15 clones G1 or G3 was assessed by Real-Time Cell Analysis. Cell index reflects growth over 24 h, and represents the average of triplicate cultures per group.

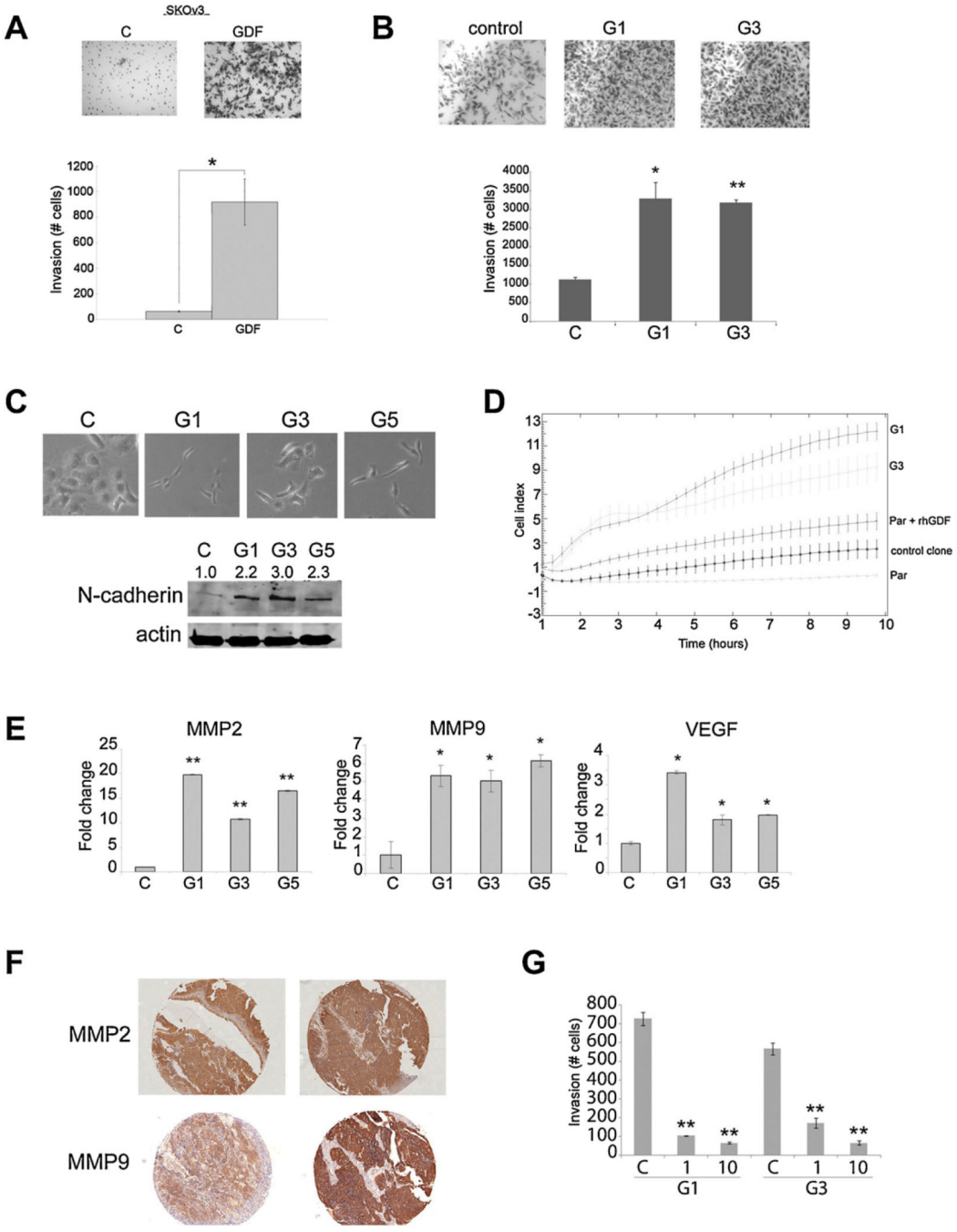

Fig. 3.

GDF15 promotes invasiveness of ovarian cancer cells. (A) SKOv3 cells were plated in Boyden chambers in the presence of 10% FBS plus vehicle control (C) or 20 ng/mL rhGDF15. (B) SKOv3 stable control clone, GDF15 stable clone 1, and GDF15 stable clone 3 cells were plated in Boyden invasion chambers in the presence of 10% FBS. For both (A) and (B), photos were taken after 24 h of invasion, and the number of invaded cells was counted in ten different fields per sample. Representative photos are shown. Values reflect the total number of invaded cells in triplicate cultures per group. (C) Representative photos

of stable control and GDF15 clones are shown at 10× magnification. Western blotting for mesenchymal marker N-cadherin was performed twice; a representative blot is shown for total cell lysates from control and GDF15 stable clones. Quantification of N-cadherin was normalized to actin, and is shown relative to control clone. (D) SKOv3, SKOv3 stable control clone, GDF15 stable clone 1, and GDF15 stable clone 3 cells were plated in the presence of 5% FBS in the upper chamber of XCelligence CIM-plates. Medium containing 10% FBS, and 20 ng/mL rhGDF15 where indicated, was placed into the plate's corresponding bottom chambers. Cell index reflects cell migration measured every 15 min for 10 h, and represents the average of triplicate cultures per group. (E) Real-time PCR was performed for invasion markers MMP-2, MMP-9, and VEGF in SKOv3 control and GDF15 stable clones 1, 3, and 5. Values reflect the fold change in transcript normalized to RPLPO housekeeping gene. (F) A tumor tissue array consisting of 122 tumor samples and 10 normal tissue samples was stained for MMP2 and MMP9. Photos were taken at 5× magnification under the microscope, and representative photos are shown. (G) SKOv3 control and GDF15 clones were plated in Boyden chambers, and treated for 24 h with DMSO (C), 1 μM (labeled "1") or 10 μM (labeled "10") of the pan-MMP inhibitor GM6001. The number of invaded cells was counted in ten different fields per sample. Values reflect the average number of invaded cells in triplicate cultures per group.

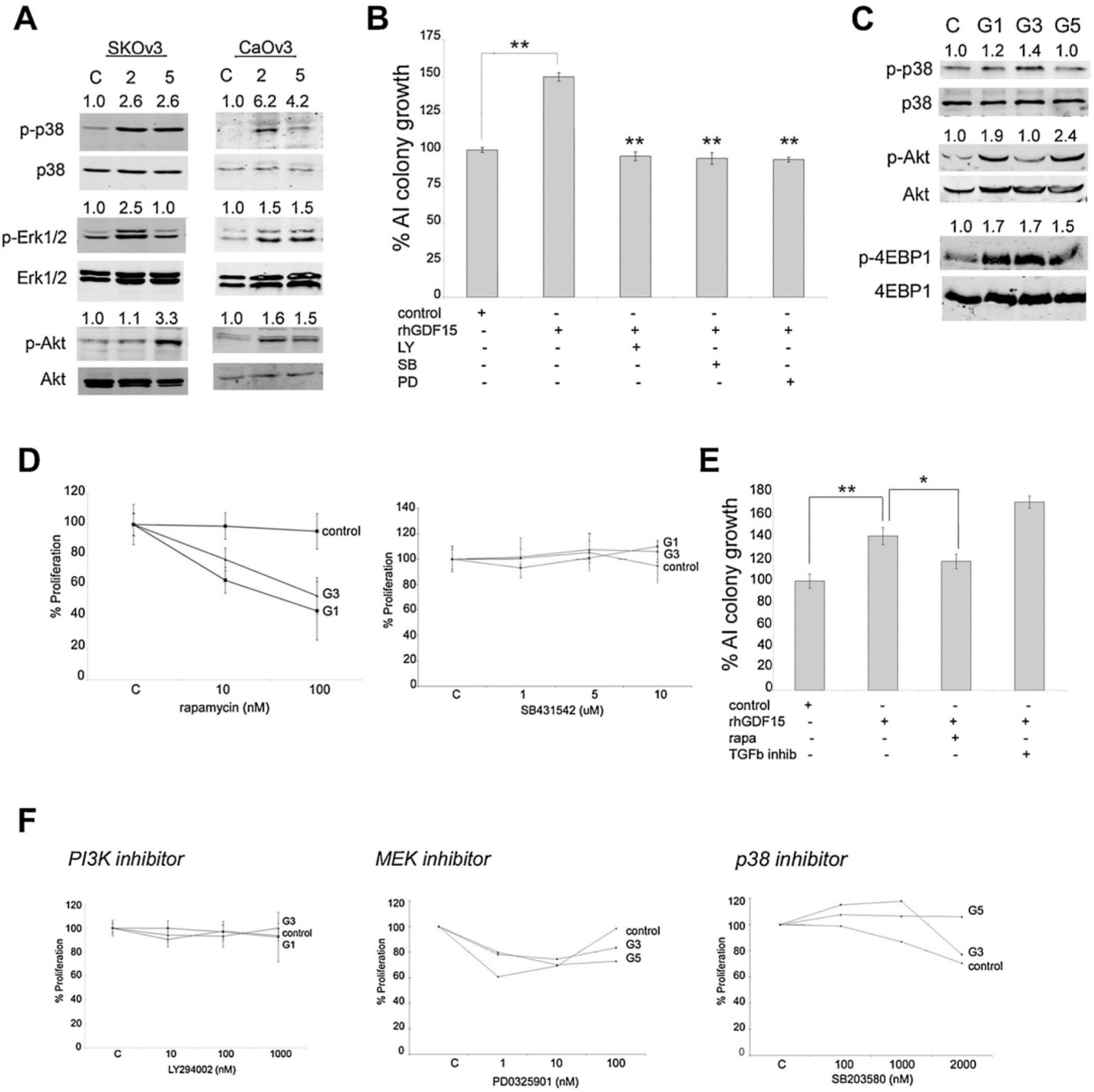

Fig. 4.

PI3K/mTORc1 and MAPK signaling are activated by GDF15 in ovarian cancer cells. (A) SKOv3 cells were serum starved overnight, and then stimulated with 20 ng/mL rhGDF15 for 2 or 5 min, or with the corresponding volume of vehicle control for 5 min. Western blots of total protein lysates were performed at least 3 times for p-Thr180/ Tyr182 p38MAPK, total p38, p-Thr202/Tyr204 p42/p44 Erk1/2, total Erk1/2, p-S473 Akt, and total Akt; representative blots are shown. Quantification is shown as a ratio of phospho-protein to total protein, and is shown relative to vehicle control. (B) SKOv3 cells were plated in matrigel.

Cells were maintained in media containing vehicle control, 20 ng/mL rhGDF15, or GDF15 plus 1 μM PI3K inhibitor LY294002, 100 nM MEK inhibitor PD0325901, or 10 μM p38MAPK inhibitor SB203580. Media and drugs were changed twice a week for 3–4 weeks. Matrigel was dissolved using dispase and cells were counted by trypan blue exclusion. Fold change in anchorage-independent (AI) growth is shown relative to the vehicle control group; $^{**}p < 0.005$ for GDF15-stimulated versus control vehicle, and for inhibitor + GDF15 groups versus GDF15 alone. (C) Total protein lysates from SKOv3 stable control and GDF15 clones 1, 3, and 5 were Western blotted at least twice for phosphorylated and total p38MAPK, Akt, and 4EBP1; representative blots are shown. Quantification is shown as a ratio of phosphorylated to total protein, and is shown relative to control clone. (D) (Left) GDF15 stable clone 1 (G1) and clone 3 (G3) and control empty vector clone cells were treated with 10 nM or 100 nM of rapamycin, or with (right) 1, 5, or 10 μM TGF beta receptor type II inhibitor SB431542. Control groups (C) were treated with DMSO alone. After 72 h, MTS proliferation assays were performed. Proliferation is shown as a percentage of the control vehicle group per cell line, and reflects the average of six replicates. (E) SKOv3 cells were plated in matrigel. Cells were maintained in media containing vehicle control, 20 ng/mL GDF15, or GDF15 plus 100 nM rapamycin or 5 μM TGF beta receptor type II inhibitor SB431542. Media and drugs were changed twice a week for 3–4 weeks. Matrigel was dissolved using dispase and cells were counted by trypan blue exclusion. Fold change in anchorage-independent (AI) growth is shown relative to the control group. (F) GDF15 stable clone 1 (G1) and clone 3 (G3) and control empty vector clone cells were treated with DMSO control (C) and the concentrations shown for LY294002, PD0325901, or SB203580. After 72 h, MTS proliferation assays were performed. Proliferation is shown as a percentage of the control vehicle group per cell line, and reflects the average of six replicates.

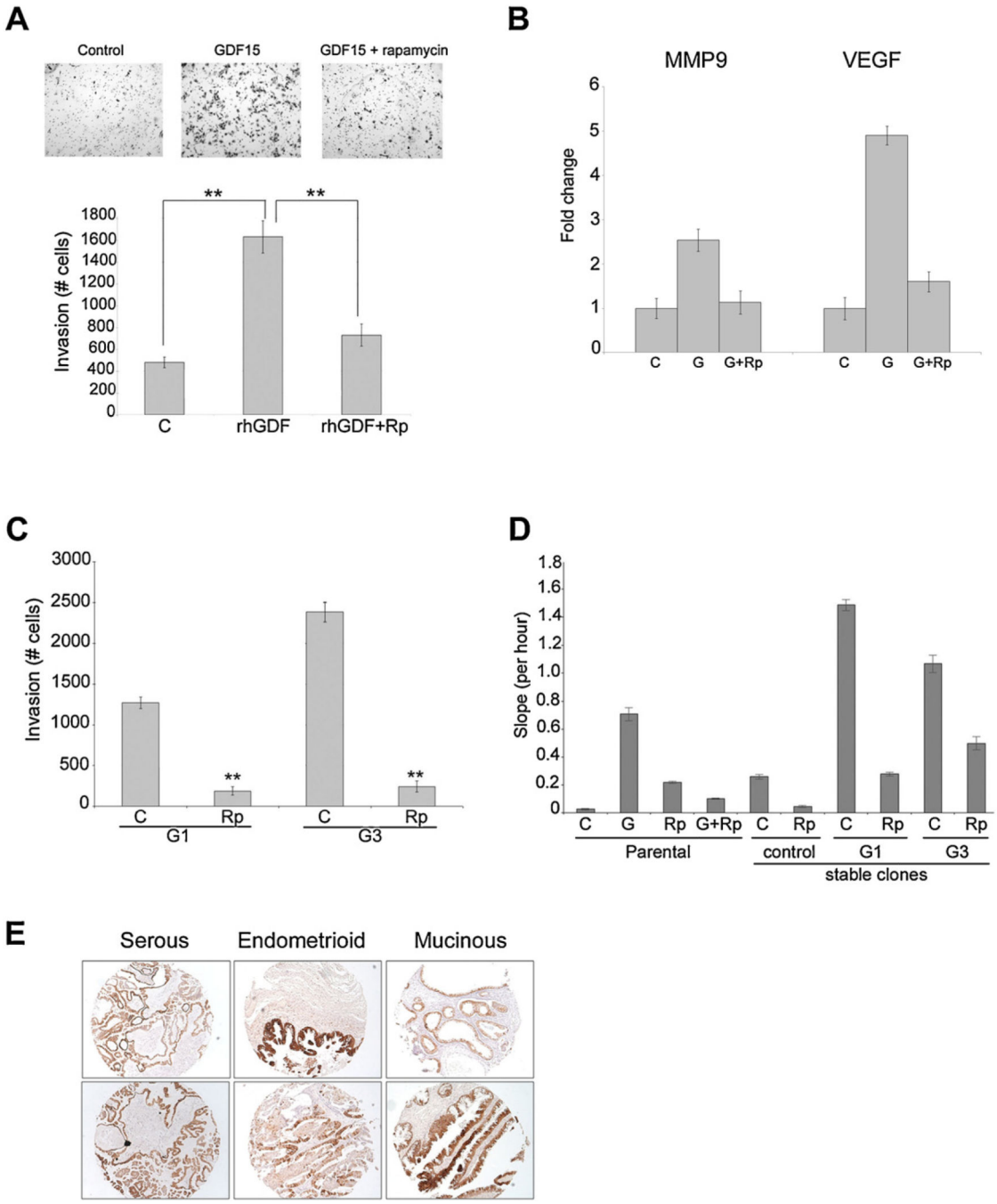

Fig. 5.

Rapamycin inhibits GDF15-mediated ovarian cancer cell invasion. (A) SKOv3 cells were plated in Boyden invasion chambers in the presence of vehicle control, 20 ng/ mL GDF15, or GDF15 plus 100 nM rapamycin (Rp). Photos were taken after 24 h of invasion (representatives shown), and the number of invaded cells was counted in ten different fields per sample. Values reflect the total number of invaded cells in triplicate cultures per group. (B) SKOv3 cells were treated with vehicle control, 20 ng/mL GDF15, or 20 ng/mL GDF15 plus 100 nM rapamycin (Rp). Real-time PCR was performed for MMP-9 and VEGF. Values

reflect the fold change in transcript normalized to RPLPO housekeeping gene. (C) SKOv3 GDF stable clones 1 and 3 were plated in Boyden invasion chambers in the presence of vehicle control (C) or 100 nM rapamycin (Rp). After 24 h of invasion, the number of invaded cells was counted in ten different fields per sample. Values reflect the total number of invaded cells in triplicate cultures per group. (D) SKOv3, SKOv3 stable control clone, GDF15 stable clone 1, and GDF15 stable clone 3 were plated in the presence of 5% FBS, and 100 nM rapamycin (Rp) where indicated, in the upper chamber of XCelligence CIM-plates. Medium containing 10% FBS, and 20 ng/mL rhGDF15 (G) where indicated, was placed into the plate's corresponding bottom chambers. CIM-plates were monitored every 15 min for 10 h. Standardized cell index (CI) values were plotted linearly against time. The CI slope per hour was calculated and is shown here as a measure of migration. Values reflect the average of triplicates at each time point.

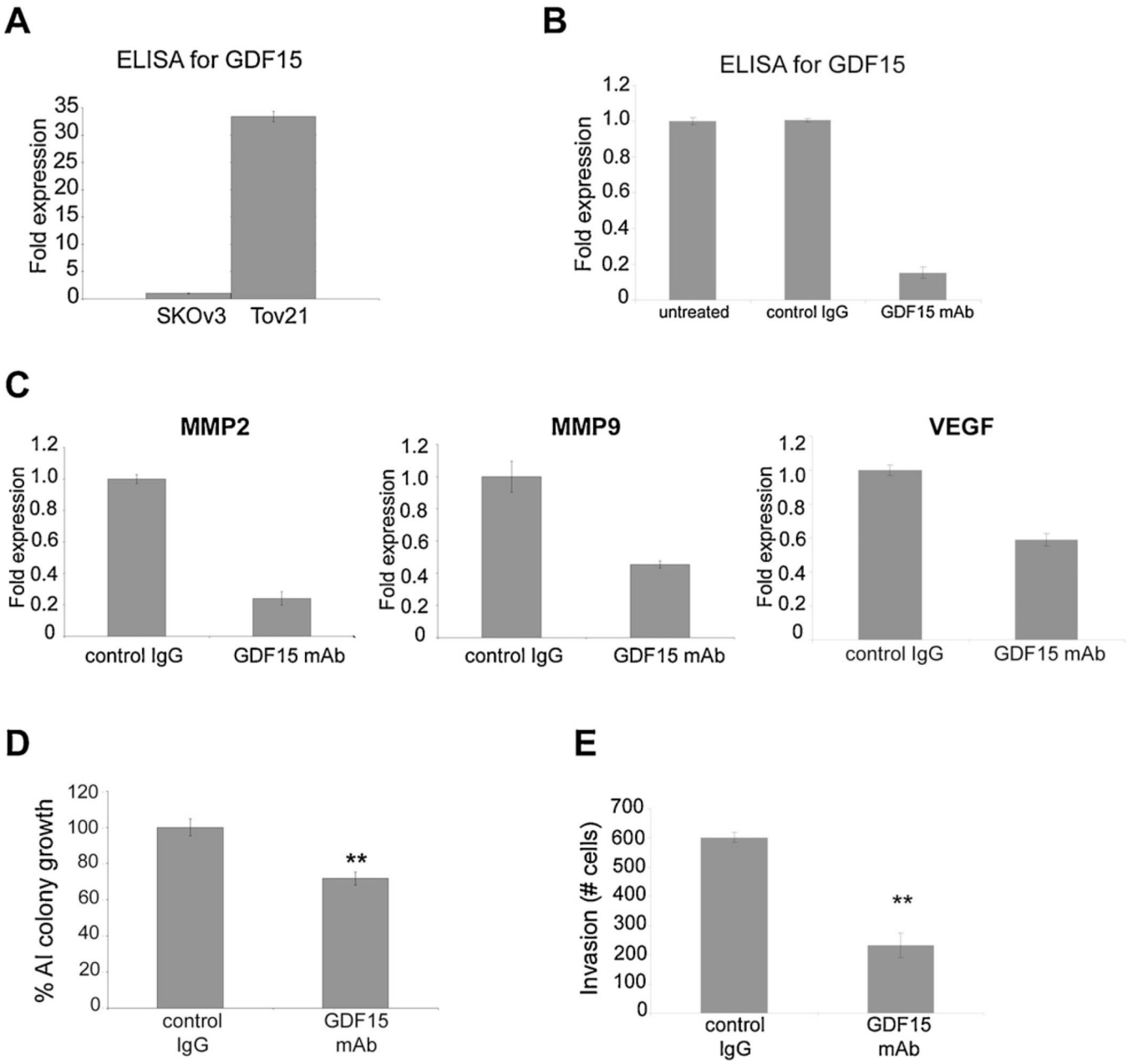

Fig. 6.

Neutralization of secreted GDF15 reduces invasion and growth of GDF15-overexpressing ovarian cancer cells. (A) Concentrations of secreted GDF15 were determined by ELISA in media from SKOv3 and Tov21 cell lines. Cells were incubated in serum-free media for 48 h prior to ELISA. Values reflect the average fold expression in three samples per group. (B) Tov21 cells were either untreated, or treated with 1 μg/mL control IgG or GDF15 mAb (147627; R&D Systems) for 24 h. The concentration of GDF15 in media was measured by ELISA in triplicates per group. Values reflect the average fold expression per group. (C) Tov21 cells were treated with 1 μg/mL control IgG or GDF15 mAb for 24 h. Real-time PCR was then performed for MMP-2, MMP-9, and VEGF, and normalized to RPLPO. Values

reflect the average fold change in normalized transcript. (D) Tov21 cells were plated in matrigel and treated with 1 μg/mL control IgG or GDF15 mAb (147627); media was changed twice a week for 3–4 weeks. Matrigel was dissolved using dispase and cells were counted by trypan blue exclusion. The percentage of anchorage-independent (AI) growth is shown relative to the control group. (E) Tov21 cells were plated in Boyden chambers and treated with 1 μg/mL control IgG or GDF15 mAb (147627). After 24 h, the number of invaded cells was counted in ten different fields per sample. Values reflect the total number of invaded cells in triplicate cultures per group.

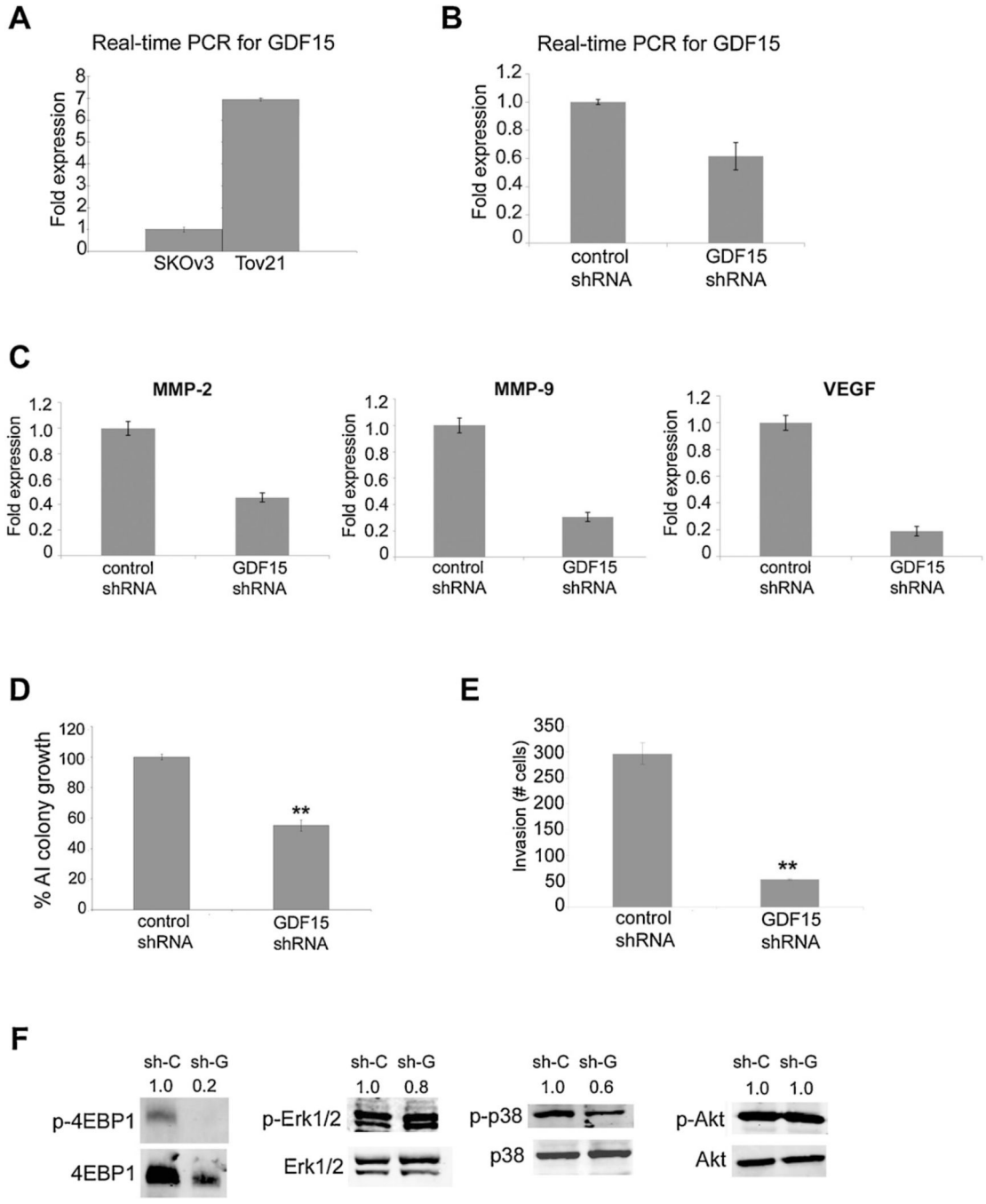

Fig. 7.

GDF15 knockdown reduces invasion and growth in association with reduced p-4EBP1 in GDF15-overexpressing ovarian cancer cells. (A) Real-time PCR was performed for GDF15 in SKOv3 and Tov21 cells, and normalized to the level of internal control transcript RPLPO. Values reflect the average fold change in normalized GDF15 transcript. (B) Tov21 cells were infected with lentiviral GDF15 shRNA or control shRNA. Real-time PCR was then performed for GDF15 and RPLPO. Values reflect the average fold change in normalized GDF15 transcript. (C) Tov21 cells were infected with lentiviral GDF15 shRNA or control

shRNA. Real-time PCR was performed for MMP-2, MMP-9, and VEGF, and normalized to RPLPO. Values reflect the average fold change in normalized transcript. (D) Tov21 cells were plated in matrigel and infected with lentiviral control or GDF15 shRNA; media and virus were changed twice a week for 3–4 weeks. Matrigel was dissolved using dispase and cells were counted by trypan blue exclusion. The percentage of anchorage-independent (AI) growth is shown. (E) Tov21 cells were plated in Boyden chambers and infected with control or GDF15 shRNA. After 24 h, the number of invaded cells was counted in ten different fields per sample. Values reflect the total number of invaded cells in triplicate cultures per group. (F) Tov21 cells were infected with lentiviral control shRNA or GDF15 shRNA for 48 h. Western blots were performed at least twice for phosphorylated and total 4EBP1, Erk1/2, p38, and Akt; representative blots are shown. Quantification is shown as a ratio of phosphorylated to total protein above each blot.

Table 1

IHC analysis of GDF15 on first ovarian tumor tissue array.

	GDF15 status			
	Negative (≤1.0)		Positive (>1.0)	
	N	%	*N*	%
Non-cancerous tissues (*n* = 5)	5	100	0	0
Ovarian cancer tissues (*n* = 29)	8	27.6	21	72.4

21 of 29 ovarian tumor tissues (~72.4%) showed positive GDF15 expression, while none of the 5 non-cancerous tissue samples showed GDF15 staining.

Table 2

IHC analysis of GDF15 according to ovarian tumor subtype on a second array.

	GDF15 status			
	Negative (≤1.0)		Positive (>1.0)	
	N	%	*N*	%
Serous (*n* = 47)	2	4.25	45	95.74
Mucinous (*n* = 24)	9	37.5	15	62.5
Endometrioid (*n* = 51)	10	19.6	41	80.39

For all subtypes, a majority of tumors showed positive GDF15 staining. In particular, the serous subtype showed the highest percentage (95.74%) of tumors with positive GDF15 staining. Collectively, 101 out of 122 (82.79%) ovarian tumor tissues stained positive for GDF15.

Table 3

IHC analysis of MMP2 and MMP9 and correlation with GDF15 expression.

GDF15	MMP2				MMP9			
	Neg (≤1.5)		Pos (>1.5)		Neg (≤1.0)		Pos (>1.0)	
	N	%	*N*	%	*N*	%	*N*	%
Negative (≤1.0) (*n* = 30)	7	23.3	23	76.7	13	43.3	17	56.7
Positive (>1.0) (*n* = 108)	8	7.4	100	92.6	6	5.6	102	94.4

123 of 138 (89.13%) of ovarian tumor tissues showed positive MMP2 staining, and 119 of 138 (86.23%) of ovarian tumor tissues showed positive MMP9 staining. GDF15 and MMP2 were significantly correlated ($p = 0.0209$, Fisher's exact), and GDF15 and MMP9 were significantly correlated ($p = 0.0001$, Fisher's exact).

Table 4

IHC analysis of p-S2448 mTOR and correlation with GDF15 expression.

GDF15	p-mTOR			
	Neg (≤1.0)		Pos (>1.0)	
	N	%	*N*	%
Negative (≤1.0) (*n* = 33)	17	51.5	16	48.5
Positive (>1.0) (*n* = 106)	33	31.1	73	68.9

89 of 139 (64%) of ovarian tumor tissues showed positive staining for p-S2448 mTOR. GDF15 and phosphorylation of mTOR were significantly correlated ($p = 0.0393$, Fisher's exact).